# Well-dispersed gallium-promoted sulfated zirconia on mesoporous MCM-41 silica

Wei Wang [a], Chang-Lin Chen [a,*], Nan-Ping Xu [a], Song Han [a], Tao Li [b], Soofin Cheng [b] and Chung-Yuan Mou [b]

[a] College of Chemical Engineering, Nanjing University of Technology, Nanjing 210009, China
[b] Department of Chemistry, National Taiwan University, 1 Roosevelt Road, Section 4, Taipei 106, Taiwan

Received 11 April 2002; accepted 11 July 2002

Gallium-promoted sulfated zirconia (SZ) was confined inside pure-silica MCM-41 (abbreviated as SZGa/MCM-41), where the latter served as a host material. It was prepared by direct dispersion of metal sulfate in the as-synthesized MCM-41 materials, followed by thermal decomposition. The SZGa/MCM-41 catalysts were characterized by XRD, $N_2$ adsorption, HRTEM, DRIFT, $NH_3$–TPD, and TPR. The experimental results showed that the ordered porous host structure was still maintained in the catalyst. SZ was in meta-stable tetragonal phase and highly dispersed on the interior surface of MCM-41 even at a high loading of 50 wt%. Additionally, a small fraction of SZ nanoparticles on the external surface of MCM-41 was obtained. The catalytic activity of SZGa/MCM-41 was examined in *n*-butane isomerization. In comparison to SZ/MCM-41 without promoter, the catalytic activities of the Ga-promoted catalysts were greatly improved. The reason proposed for the higher activity of the Ga-promoted catalysts was that Ga enhances the oxidizing ability of the catalysts.

**KEY WORDS:** Ga-promoted sulfated zirconia; MCM-41; butane isomerization.

## 1. Introduction

Mesoporous materials with highly ordered pore structures have potential applications in catalysis, sorption, and as nanostructured host/guest compounds because of their high surface areas, large pore volume and tunable uniform pore structures [1]. However, the silica walls of mesoporous materials are quite neutral and the molecular sieves themselves have little use without proper modification on the wall. Many efforts have been devoted to the introduction of some heteroatoms such as Al [2] into the silicate framework, or the introduction of encapsulation of solid acids such as heteropoly acids [3] into MCM-41 channels to generate acidic sites.

In recent years, SZ and related materials have attracted increasing attention because they were found to be highly active in catalyzing reactions of industrial importance, such as hydrocarbon isomerization. However, the non-uniform pore size and relatively small surface area of these catalysts may limit their applications for catalyzing bulky molecules. Therefore, a composite material of SZ and meso-porous silica should greatly expand the catalytic capabilities of the material. Several papers have been published on the preparation and applications of SZ supported on various meso-porous silica [4–9].

* To whom correspondence should be addressed.
E-mail: changlinc@yahoo.com

Recently, it was reported that doping the SZ with various metals such as Fe, Mn [10], and Al [11–19] would enhance their catalytic activity in the *n*-butane isomerization reaction. In the present work, the research is focused on the synthesis of Ga-promoted SZ by using MCM-41 as host materials. The method is by direct dispersion of metal sulfate in the as-synthesized MCM-41 materials. The textural properties of SZGa/MCM-41 were characterized by XRD, $N_2$ adsorption, and HRTEM. Experiments show that the procedure leads to highly dispersed SZ onto the external and internal surfaces of MCM-41. The catalytic activities of SZGa/MCM-41 in *n*-butane isomerization were investigated. In comparison with SZ/MCM-41, the catalytic activity of SZGa/MCM-41 was improved greatly. The reasons for the higher activity of the promoted catalysts were discussed.

## 2. Experimental

### 2.1. Catalyst preparation

As-synthesized pure siliceous MCM-41 was prepared according to the literature [20]. The as-synthesized mesoporous material was slurry impregnated with a desired amount of $Zr(SO_4)_2$ in methanol slurry and stirred at room temperature for about 10 h. The resulting sample was dried at 80 °C. Finally, it was calcined at a desired temperature for 3 h in air. Ga-promoted samples were prepared in the same way with the desired amounts of $Zr(SO4)_2$ and $Ga_2(SO4)_3$ mixed as methanol slurry.

1011-372X/02/1100-0281/0 

### 2.2. Catalyst characterization

XRD patterns of the samples were obtained on a Bruker D8 Advance instrument with Cu $K_\alpha$ radiation at 40 kV and 30 mA. The surface-area and pore-size distribution measurements were carried out on a Micromeritics ASAP 2010 automatic adsorption instrument using $N_2$ as the analysis gas. DRIFT spectra of the samples were acquired as previously described [18]. HRTEM was performed on a CM-200 Philips, with an operating voltage of 200 keV. TPR and $NH_3$-TPD experiments were performed on a CHEMBET-3000, equipped with a thermal conductivity detector (TCD). TPR profiles were recorded in 10% $H_2$/Ar of 30 ml/min from 100 °C to 700 °C at 10 °C/min, while $NH_3$–TPD profiles were recorded in an He flow of 30 ml/min from 100 °C to 600 °C at 10 °C/min. Sulfur content in the catalysts was detected by a chemical method. The sulfate was turned into $BaSO_4$ and determined by a gravimetric method.

### 2.3. Catalytic experiments

The catalytic activity of samples was tested in an *n*-butane isomerization reaction using a fixed-bed continuous flow reactor. The reactor was operated at atmospheric pressure. 0.6 g of the catalyst was loaded into the reactor and then pretreated in flowing dry air (20 ml/min) at 450 °C for 3 h. The reactor temperature was then lowered to the reaction temperature of 250 °C. The feed gas *n*-butane/$H_2$ mixtures (1 : 10 v/v) flowed through the catalyst bed at an *n*-butane WHSV of 0.52 $h^{-1}$. An on-line SP6800A gas chromatograph equipped with FID was used to analyze the reaction products.

## 3. Results and discussion

### 3.1. X-ray diffraction

Figure 1 shows the powder XRD patterns of SZGa/MCM-41 after different heating treatment. All samples show a diffraction peak due to (100) reflection at low $2\theta$ ranges, which are characteristic of an ordered porous structure. An increase in the intensity of the (100) reflection with an increase in calcination temperature was observed (figure 1). This may be due to the removal of the organic component and decomposition of metal sulfate in the pores. The XRD patterns (figure 1(1)) for uncalcined samples within the range of 10–70 °C show no peaks. This indicates that the metal sulfate may have been rather homogeneously dispersed onto the interior surfaces of MCM-41. Figure 1(2), (3), and (4) show that very weak and broad peaks in the higher $2\theta$ range appeared, which can be indexed into the presence of the tetragonal $ZrO_2$ crystalline phase. This suggests that very small SZ particles might be formed outside

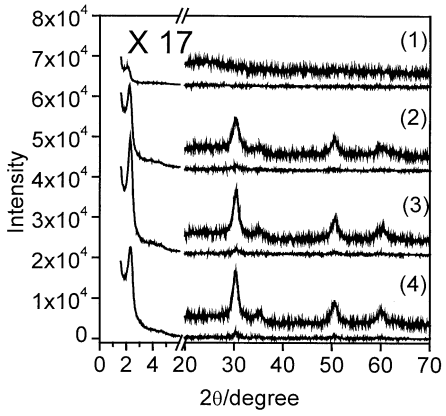


Figure 1. XRD patterns of the composites of SZGa/MCM-41 ($ZrO_2$: 50 wt%, Ga: 1.7 wt%) calcined at various temperatures. (1) 80 °C; (2) 630 °C, 3 h; (3) 680 °C, 3 h; (4) 720 °C, 3 h.

the pore structure when the sample was further heated at or above 630 °C. Since particles of these dimensions are observable by XRD, the very small peaks of $ZrO_2$ observed in the region of 10–70° implied that their concentration was relatively low, and most of the SZ was highly dispersed on the interior surface of MCM-41 at a high loading of 50 wt% SZ.

### 3.2. Physico-chemical properties of the samples

Figure 2 illustrates the $N_2$ adsorption/desorption isotherm and pore-size distribution of SZGa/MCM-41 in comparison to those of pristine MCM-41. The $N_2$ adsorption amount decreased and the inflection point of the respective steps is shifted to lower values of $P/P_0$, as expected for smaller pores. It is also noticeable that the pore-size distribution remains narrow for SZGa/MCM-41. These results indicate that the supported SZ has been well dispersed onto the interior surface of MCM-41. Table 1 shows the sulfur content, BET surface area, and total pore volume of series SZGa/MCM-41 samples. It is noticed that the BET surface area and pore volume reduce with the deposition of SZ-modified samples in comparison to that of parent MCM-41.

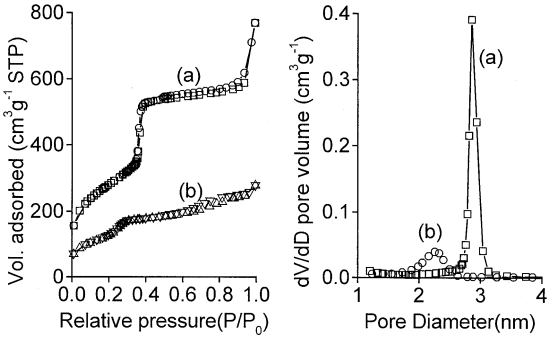


Figure 2. $N_2$ adsorption/desorption isotherms and pore-size distribution curves of (a) MCM-41, and (b) calcined SZGa/MCM-41 ($ZrO_2$: 50 wt%, Ga: 1.7 wt%).

Table 1
Physico-chemical properties of the catalysts and support.

| Catalysts | Ga content (wt%) | Calc. temp. (°C) | S content (wt%) | BET S.A. ($m^2$/g) | Pore volume (ml/g) |
|---|---|---|---|---|---|
| SZ/MCM-41 [a] | 0.0 | 680 | 0.91 | 442 | 0.31 |
| SZGa/MCM-41 [a] | 0.57 | 680 | 1.26 | 438 | 0.32 |
| SZGa/MCM-41 [a] | 1.7 | 680 | 1.45 | 480 | 0.36 |
| SZGa/MCM-41 [a] | 2.84 | 680 | 1.63 | 357 | 0.27 |
| SZGa/MCM-41 [a] | 1.7 | 630 | 2.19 | 442 | 0.31 |
| SZGa/MCM-41 [a] | 1.7 | 720 | 0.63 | 350 | 0.26 |
| MCM-41 | – | 680 | – | 1010 | 1.10 |

[a] Samples contain 50 wt% $ZrO_2$.

However, the surface area and pore volumes of SZGa/MCM-41 samples are still much larger than those of the traditional SZ (around 100–120 $m^2$/g [21]). Both Ga content and calcination temperature affect the surface area. For SZGa/MCM-41 catalysts calcined at 680 °C, the BET surface area increases to 480 $m^2$/g with the addition of a proper amount of Ga. It can also be seen that the sulfur content decreases as the calcination temperature increases. In contrast, the sulfur content increases with the addition of Ga. It may be explained that the addition of Ga may help to stabilize the surface sulfate species during calcinations at 680 °C.

Figure 3 shows the HRTEM picture of SZGa/MCM-41 after calcination at 680 °C. From the HRTEM micrograph of SZGa/MCM-41, well-ordered channels with continuous walls are clearly observed. On the other hand, some external SZ particles were in fact present and the dispersed particles were observed around 10 nm. It is clear that the sizes of SZ particles on the outside surface exceeded the sum of the pore diameter and the wall thickness. It can be concluded that the use of elevated temperature leads to the premature formation of large SZ particles outside of the pores. However, the dispersed particles or layers formed in the channels of MCM-41 are very small. Porous MCM-41 gives a physical constraint to prevent the formation of large SZ agglomerates. To confirm the presence of SZ in the channels of MCM-41, the DRIFT spectra of MCM-41 and SZGa/MCM-41 calcined at 680 °C were shown in figure 4. The spectra were taken after the samples were heated at 300 °C for 1 h. Two strong absorption peaks at 1344 $cm^{-1}$ and at 3740 $cm^{-1}$ are observed for MCM-41, which correspond to the Si–O stretching vibration and the O–H vibration associated with the free SiO–H groups, respectively. Upon supporting SZ on MCM-41, the intensity of both peaks was markedly reduced. The decreased absorbance is presumably due to the dispersion of SZ on MCM-41 and the chemical interaction of SZ with silanols.

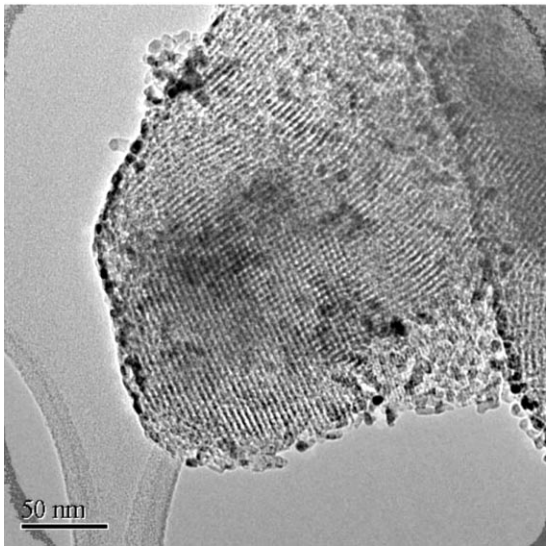


Figure 3. HRTEM image of SZGa/MCM-41 calcined at 680 °C ($ZrO_2$: 50 wt%, Ga: 1.7 wt%).

### 3.3. Acidity measurements

The $NH_3$–TPD is a simple method widely used to investigate both the strength and the number of acid sites present on the surface of acid solid. The $NH_3$–TPD profiles of the SZ/MCM-41 and SZGa/MCM-41 samples after calcination at 680 °C are shown in figure 5. They present only one wide peak of desorption at about 250 °C. Clearly, the strength of acid sites present on SZ/MCM-41 is not affected by the presence of Ga.

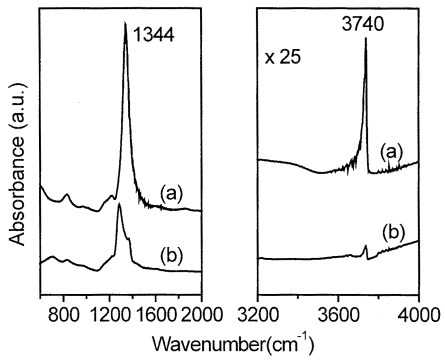


Figure 4. DRIFT spectra of samples calcined at 680 °C after the powder samples were heated at 300 °C for 1 h. (a) Calcined MCM-41; (b) SZGa/MCM-41 ($ZrO_2$: 50 wt%, Ga: 1.7 wt%).

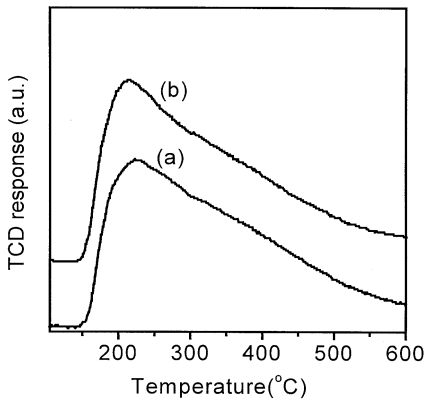


Figure 5. TPD profiles of samples calcined at 680 °C. (1) SZ/MCM-41 ($ZrO_2$: 50 wt%); (2) SZGa/MCM-41 ($ZrO_2$: 50 wt%, Ga: 1.7 wt%).

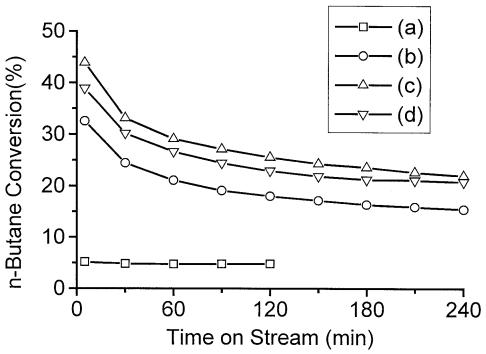


Figure 7. Catalytic activity of catalysts calcined at 680 °C at constant $ZrO_2$ content 50 wt% with various Ga contents. (a) 0.0 wt%; (b) 0.57 wt%; (c) 1.7 wt%; (d) 2.84 wt%.

### 3.4. TPR of SZ/MCM-41 and SZGa/MCM-41

Two representative examples of TPR profiles are shown in figure 6. The SZ/MCM-41, calcined at 680 °C, displays a reduction peak starting at 550 °C with the maximum centered at 660–670 °C. Conversely, SZGa/MCM-41 calcined at 680 °C displays a reduction peak starting at 450 °C with the maximum centered at 528 °C. Blank experiments confirmed no thermal decomposition of sulfates before a temperature of 700 °C. This suggests that the presence of Ga influences the oxidizing ability of SZGa/MCM-41.

### 3.5. Catalytic activity in n-butane isomerization

Figure 7 showed the effect of various amounts of Ga incorporated in SZ/MCM-41 on *n*-butane isomerization at 250 °C. The activity of the SZ/MCM-41 was much lower. The selectivity to isobutane for Ga-free catalyst is about 78%. The addition of a small amount of Ga can greatly improve the catalytic activity, and the selectivity to isobutene for all the Ga-promoted catalysts increases to around 88%. The *n*-butane conversion increased with the Ga content up to 1.7 wt%, and then decreased as the Ga content was further increased. It may be explained that excess amounts of Ga may cover the zirconia surface and reduce the catalytically active sites. It is also observed that the steady activity values of these SZGa/MCM-41 samples are still higher than that of the SZ/MCM-41, though the initial deactivation was fast. The catalysts after reaction on stream for 6 h can be regenerated in dry air at 450 °C for 3 h. It seems that the deactivation is due to the coking deposited on the catalyst surface.

The calcination temperature used for preparation of SZGa/MCM-41 catalysts has a significant effect on the catalytic activities of *n*-butane isomerization, as shown in figure 8. The initial conversion of the catalyst calcined at 680 °C was higher than those of the catalysts calcined at 630 °C and 720 °C. When the calcination temperature is at 630 °C, which is lower than the decomposition temperature of $Zr(SO4)_2$ and $Ga_2(SO4)_3$, $Zr(SO4)_2$ and $Ga_2(SO4)_3$ are partly decomposed. When the calcination temperature is at 720 °C, the amount of surface sulfated ions decreases markedly.

We try to relate the characterization study of these catalysts with the catalytic properties in order to understand the Ga promoter effect for *n*-butane isomerization.

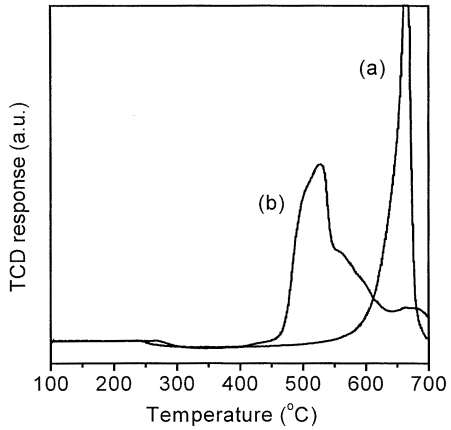


Figure 6. TPR profiles of samples calcined at 680 °C. (1) SZ/MCM-41 ($ZrO_2$: 50 wt%); (2) SZGa/MCM-41 ($ZrO_2$: 50 wt%, Ga: 1.7 wt%).

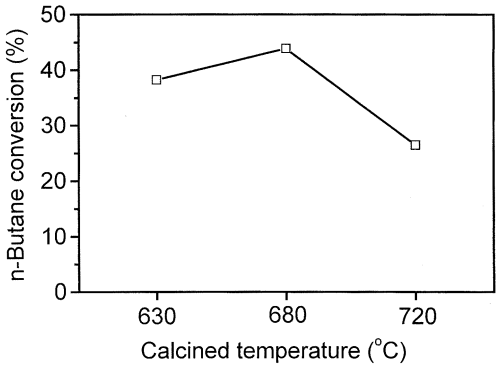


Figure 8. Effect of calcination temperature on butane conversion at time-on-stream of 5 min over SZGa/MCM-41 at 250 °C ($ZrO_2$: 50 wt%, Ga: 1.7 wt%).

In the literature, there are several attempts to correlate the acidity with the catalytic performance of SZ. In our case, nevertheless, the acidity characterization of the samples shows no difference in strength of the acid sites between SZ/MCM-41 and SZGa/MCM-41. The TPR profiles indicate that Ga enhances the oxidizing ability of SZGa/MCM-41. These results would favor the idea that SZ/MCM-41 is a bifunctional catalyst for *n*-butane isomerization, containing acid functionality and redox functionality [22]. It is worth noting, from TPR data, that the sulfate reduction does not occur in the temperature range where the *n*-butane reaction occurs. The remarkable activity of SZGa/MCM-41 is due to the enhanced redox capability.

## 4. Conclusions

In this work, Ga-promoted SZ can be well dispersed in the channels of MCM-41. All SZGa/MCM-41 samples display a narrow mesopore size distribution. On the other hand, under high $ZrO_2$ loading, some SZ clusters are dispersed outside the MCM-41 structure. The proper addition of Ga enhanced the catalytic activity and product selectivity for *n*-butane isomerization. The best Ga loading in these catalysts calcined at 680 °C is around 1.7 wt%. The Ga promoter is postulated to improve the redox capability of SZGa/MCM-41.

## Acknowledgment

We acknowledge the support of the Educational Department of Jiangsu Province project (00KJB530001 to C.-L.C.) and the Key Laboratory of Chemical Engineering and Technology of Jiangsu Province. We thank Dr. H.-P. Lin for conducting the HRTEM observations. We also thank the CTCI foundation for doing the HRTEM observations.

## References

[1] C.T. Kresge, M.E. Leonowicz, W.J. Roth, J.C. Vartuli and J.S. Beck, Nature 359 (1992) 710.
[2] A. Corma, M.J. Climent, S. Iborra, M.C. Nawarro and J. Primi, J. Catal. 161 (1994) 569.
[3] I.V. Kozhevnikov, A. Sinnema, R.J.J. Jansen, K. Pamin and H. van Bekkum, Catal. Lett. 30 (1995) 241.
[4] T. Lei, W.M. Hua, Y. Tang, Y.H. Yue and Z. Gao, Chem. J. Chinese Univ. 21 (2000) 1240.
[5] Q.H. Xia, K. Hidajat and S. Kawi, Chem. Commun. (2000) 2229.
[6] C.L. Chen, S. Cheng, H.P. Lin, S.T. Wong and C.Y. Mou, Appl. Catal. A 215 (2001) 21.
[7] Q.H. Xia, K. Hidajat and S. Kawi, J. Catal. 205 (2002) 318.
[8] W.M. Hua, Y.H. Yue and Z. Gao, J. Mol. Catal. A 170 ( 2001) 195.
[9] H. Matsuhashi, M. Tanaka, H. Nakamura and K. Arata, Appl. Catal. A 208 (2001) 1.
[10] C.Y. Hsu, C.R. Heimbuch, C.T. Armes and B.C. Gates, J. Chem. Soc. Chem. Commun. (1992) 1645.
[11] S. Baba, Y. Shibata, T. Kawamura, H. Takaoka, T. Kimura, K. Kousaka, Y. Minato, N. Yokoyama, K. Lida and T. Imai, Eur. Patent 174836, 1985.
[12] M. Marella, M. Tomaselli, L. Meregalli and F. Pinna, Eur. Patent 983967, 2000.
[13] Z. Gao, Y. Xia, W. Hua and C. Miao, Topics Catal. 6 (1998) 101.
[14] T. Lei, J.S. Xu, W.M. Hua, Y. Tang and Z. Gao, Catal. Lett. 61 (1999) 213.
[15] T. Lei, J.S. Xu, Y. Tang, W.M. Hua and Z. Gao, Appl. Catal. A 192 (2000) 181.
[16] E. Angelescu, M. Ropot, F. Contantinescu, D. Boiangiu and M. Pencea, Prog. Catal. 7 (1998) 5.
[17] J.A. Moreno and G. Poncelet, J. Catal. 203 (2001) 453.
[18] C.L. Chen, T. Li, S. Cheng, H.P. Lin, C. J. Bhongale and C.Y. Mou, Microporous Mesoporous Mater. 50 (2001) 201.
[19] C.L. Chen, T. Li, S. Cheng, N.P. Xu and C.Y. Mou, Catal. Lett. 78 (2002) 223.
[20] H.P. Lin, S. Cheng and C.Y. Mou, Microporous Mater. 10 (1997) 111.
[21] B.H. Davis, R.A. Keogh and R. Srinivasan, Catal. Today 20 (1994) 219.
[22] S.X. Song and R.A. Kydd, Catal. Lett. 51 (1998) 95.